



Published in final edited form as:

Cell Rep. 2022 January 18; 38(3): 110255. doi:10.1016/j.celrep.2021.110255.

Presynaptic mechanisms underlying GABA_B-receptor-mediated inhibition of spontaneous neurotransmitter release

Baris Alten^{1,2}, Natalie J. Guzikowski^{1,2}, Zack Zurawski¹, Heidi E. Hamm¹, Ege T. Kavalali^{1,2,3,*}

¹Department of Pharmacology, Vanderbilt University, 7130A MRB III 465 21st Avenue South, Nashville, TN 37240-7933, USA

²Vanderbilt Brain Institute, Vanderbilt University, Nashville, TN 37240-7933, USA

³Lead contact

SUMMARY

Inhibition of neurotransmitter release by neurotransmitter substances constitutes a fundamental means of neuromodulation. In contrast to well-delineated mechanisms that underlie inhibition of evoked release via suppression of voltage-gated Ca²⁺ channels, processes that underlie neuromodulatory inhibition of spontaneous release remain unclear. Here, we interrogated inhibition of spontaneous glutamate and GABA release by presynaptic metabotropic GABA_B receptors. Our findings show that this inhibition relies on Gβγ subunit action at the membrane, and it is largely independent of presynaptic Ca²⁺ signaling for both forms of release. In the case of spontaneous glutamate release, inhibition requires Gβγ interaction with the C terminus of the key fusion machinery component SNAP25, and it is modulated by synaptotagmin-1. Inhibition of spontaneous GABA release, on the other hand, is independent of these pathways and likely requires alternative Gβγ targets at the presynaptic terminal.

Graphical Abstract

This is an open access article under the CC BY-NC-ND license (<http://creativecommons.org/licenses/by-nc-nd/4.0/>).

*Correspondence: ege.kavalali@vanderbilt.edu.

AUTHOR CONTRIBUTIONS

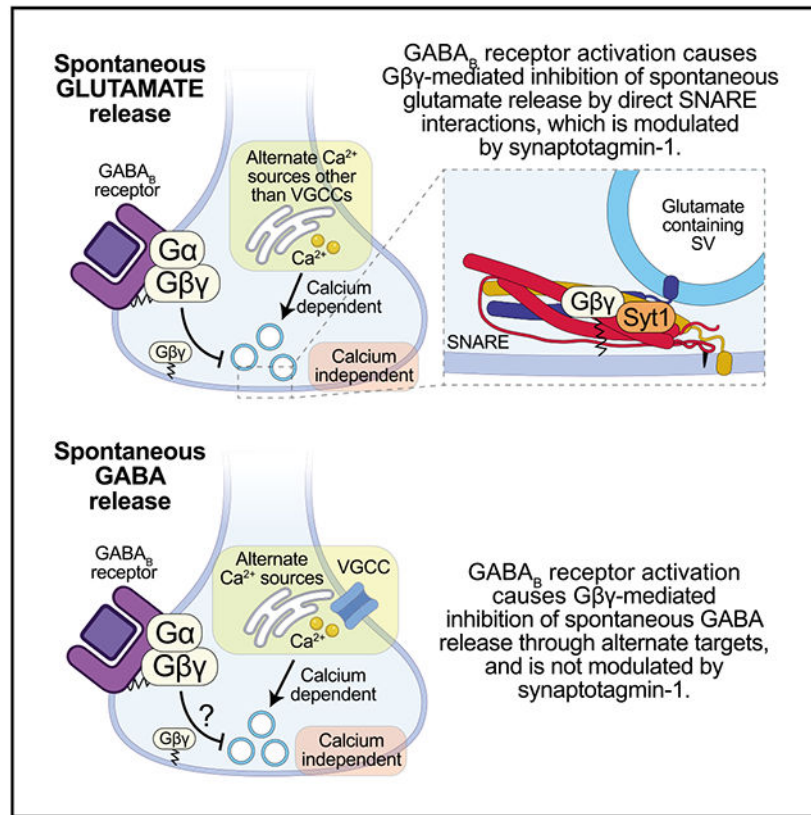
B.A. prepared primary neuronal cultures, performed whole-cell voltage-clamp experiments, performed western blotting, prepared the figures, and wrote the initial draft of the manuscript. N.J.G. prepared primary neuronal cultures, performed live Ca²⁺ imaging (from acquisition to analysis), performed whole-cell voltage-clamp experiments, performed western blotting, prepared figures, and edited the manuscript. Z.Z. and H.E.H. provided SNAP25^{-/-} mice. H.E.H. provided insight into the design of the study. E.T.K. supervised the project, edited the manuscript, and worked with B.A. in overall design and direction of the project.

SUPPLEMENTAL INFORMATION

Supplemental information can be found online at <https://doi.org/10.1016/j.celrep.2021.110255>.

DECLARATION OF INTERESTS

The authors declare no competing interests.



In brief

Alten et al. demonstrate how metabotropic GABA_B receptors utilize Gβγ subunits to differentially regulate spontaneous excitatory and inhibitory neurotransmitter release. Their study identifies key Gβγ-mediated signaling pathways that target spontaneous neurotransmitter release.

INTRODUCTION

Inhibition of synaptic transmission by secreted neurotransmitter substances is a ubiquitous form of neuromodulation across diverse neuronal circuits (Dunlap and Fischbach, 1978). A well-established mechanism for this form of neuromodulation involves activation of presynaptic G-protein-coupled receptors (GPCRs) and subsequent direct suppression of presynaptic voltage-gated Ca²⁺ channel (VGCC) gating by Gβγ subunits (Figures 1A and 1B; Bean, 1989; Herlitze et al., 1996; Ikeda, 1996; Lipscombe et al., 1989). Although this mechanism can largely account for inhibition of action-potential-triggered evoked neurotransmitter release (Figures 1A and 1B), it remains unclear whether a similar inhibition of spontaneous release exerted by certain neuromodulatory substances is governed by the same mechanism (Dittman and Regehr, 1996; Scanziani et al., 1992). There is evidence that some spontaneous release events are elicited by spontaneous openings of presynaptic VGCCs (Ermolyuk et al., 2013; Williams et al., 2012; Williams and Smith, 2018), while an equally significant fraction resists blockade of VGCCs, suggesting a role for either

non-canonical presynaptic Ca^{2+} signaling pathways or signaling cascades independent of intracellular Ca^{2+} (Figure 1B; Chanaday et al., 2021; Kavalali, 2015).

In this study, we aimed to address the mechanism by which neurotransmitters inhibit spontaneous release by focusing on a well-documented effect of presynaptic GABA_B receptor activation on resting glutamatergic and GABAergic transmission in hippocampal synapses. GABA_B receptors are GPCRs, which are formed as obligate heterodimers of GABA_{B1} and GABA_{B2} subunits (White et al., 1998). Upon activation with either GABA or baclofen, a conformational transition triggers the exchange of guanosine diphosphate (GDP) for guanosine triphosphate (GTP) in $G_i\alpha$, dissociating GTP-bound active $G_i\alpha$ from $G\beta\gamma$ (Frangaj and Fan, 2018). While GTP- $G_i\alpha$ constitutes the main signal transducer by inhibiting adenylyl cyclase to decrease cyclic AMP (cAMP) concentrations, free $G\beta\gamma$ can also act as a secondary messenger by gating G-protein-activated inward rectifying K^+ channels (GIRK) and inhibiting VGCCs (Holz et al., 1986; Luscher and Slesinger, 2010; Tedford and Zamponi, 2006).

Our results suggest a key membrane de-limited role for $G\beta\gamma$ subunits in inhibition of both spontaneous glutamate and GABA release. Although activation of GABA_B receptors partially inhibited occasional spontaneous presynaptic Ca^{2+} transients, strong chelation of intracellular Ca^{2+} largely spared the degree of inhibition while decreasing the baseline rate of spontaneous release, suggesting a dominant role for Ca^{2+} -independent mechanisms. Glutamatergic synapses harboring a mutant form of SNARE (soluble NSF attachment protein receptor) protein, SNAP-25, where its last three amino acids are deleted, prevented significant inhibition of spontaneous glutamate release by baclofen, while inhibition of spontaneous GABA release remained unaffected by the same mutation. Interestingly, loss of function of synaptotagmin-1 resulted in substantial augmentation of spontaneous release and also potentiation of GABA_B -receptor-mediated inhibition of spontaneous glutamate release without affecting inhibition of GABA release. Taken together, these data suggest an essential role for $G\beta\gamma$ -SNARE machinery interactions modulated by synaptotagmin-1 in GABA_B -receptor-mediated inhibition of spontaneous glutamate release. GABAergic spontaneous events, on the other hand, are susceptible to $G\beta\gamma$ -mediated inhibition via targets alternative to aforementioned molecules.

RESULTS

Scavenging $G\beta\gamma$ attenuates GABA_B -receptor-mediated inhibition of spontaneous release

We utilized primary dissociated hippocampal cultures and recorded miniature excitatory or inhibitory postsynaptic currents (mEPSCs or mIPSCs) with whole-cell voltage-clamp electrophysiology in the presence of tetrodotoxin (TTX) to block action potentials. Perfusion of 10 μM baclofen rapidly and consistently reduced the frequency of both mEPSCs and mIPSCs without altering their amplitudes throughout our study, suggesting a presynaptic origin of action consistent with what has been reported previously. Given the role of $G\beta\gamma$ in inhibition of evoked neurotransmitter release (Blackmer et al., 2001), we tested whether $G\beta\gamma$ is also implicated in inhibition of spontaneous release upon activation of GABA_B receptors with baclofen. For this purpose, we tried to scavenge $G\beta\gamma$ with a C-terminal fragment of GPCR kinase 2 (ct-GRK2) (Blackmer et al., 2001), which corresponds to

amino acids 548–671 of bovine homolog of GRK2 (Figure 1C). This fragment consists of the $G\beta\gamma$ -binding PH domain of GRK2. We cloned ct-GRK2 into an expression vector, which was packed into lentiviral particles to infect neuronal cultures on 4th day *in vitro* (DIV 4). In between DIV 14 and 18, when the expression of ct-GRK2 had plateaued (Figure 1D), we recorded mEPSCs before and during 10 μ M baclofen perfusion (Figure 1E). ct-GRK2 expression resulted in mild attenuation of baclofen's inhibitory effect on mEPSC frequency, albeit failed to reach statistical significance (Figure 1E). Given that $G\beta\gamma$ is membrane localized, we decided to clone the N-myristoylation signaling peptide of Src to the N terminus of ct-GRK2 to anchor it to the plasma membrane, where scavenging efficacy is expected to be greater (Figure 1F; Rishal et al., 2005). Similar to ct-GRK, myristoylated ct-GRK2 (myr ct-GRK2) was expressed by neurons upon infection with lentiviral particles containing the expression vector (Figure 1G). Expression of myr ct-GRK2 significantly halved the baclofen-mediated inhibition of mEPSC frequency (Figures 1H and 1I), implicating $G\beta\gamma$ as the mediator as well as the vicinity of plasma membrane as the location of action. The same effect was observed also for mIPSCs (Figures 1J and 1K), suggesting $G\beta\gamma$ functions as the effector of inhibition of both spontaneous glutamate and GABA release. Interestingly, the expression of myr ct-GRK2 caused a significant decrease in mIPSC frequency at baseline (Figure 1J), whereas no significant change was observed for mEPSC frequency (Figure 1H). To investigate the possible tonic inhibition on spontaneous release by constitutive GABA_B receptor activation, we perfused with 200 μ M saclofen, a GABA_B receptor antagonist, while recording mEPSCs and mIPSCs. Saclofen perfusion did not cause any changes in frequencies of mEPSCs or mIPSCs (Figure 1L). In addition, we also tested the effect of another GABA_B receptor antagonist, CGP-55845, directly following perfusion and with a 10-min application. There was no change in spontaneous event frequency, further demonstrating no tonic role of GABA_BR regulation in our system (see Table S1).

Baclofen inhibits spontaneous release in Ca²⁺-dependent and -independent manners

Presynaptically, direct binding of $G\beta\gamma$ to VGCCs to inhibit evoked Ca²⁺ currents is considered as the main mechanism of inhibiting evoked neurotransmitter release (De Waard et al., 1997; Herlitz et al., 1996; Holz et al., 1986). Measurement of Ca²⁺ currents both electrophysiologically (Takahashi et al., 1998) and with optical probes (Dittman and Regehr, 1996) showed baclofen-mediated inhibition of the action-potential-triggered Ca²⁺ transients. However, it is not known whether the same inhibition applies to spontaneous Ca²⁺ transients, which partially drive the spontaneous neurotransmitter release (see also Figure 1B; Williams and Smith, 2018). Here, we used a genetically encoded optical Ca²⁺ probe, GCaMP6s, attached to the vesicular SNARE synaptobrevin-2 (syb2) (Figure 2A), to measure spontaneous presynaptic miniature Ca²⁺ transients (pmSCTs) in the presence of TTX to block action potential firing. Synaptic regions of interest (ROIs) were selected to analyze the frequency and amplitude of transient changes in fluorescence intensity before and during baclofen perfusion (Figure 2B). pmSCTs with a peak amplitude greater than four standard deviations above the average baseline fluorescence signal were included for analysis to ensure that only transient increases in fluorescent signal representing local changes in Ca²⁺ concentration were detected and not noise (Figure 2C). In this setting, we detected pmSCTs in up to 10% syb2-GCaMP6s labeled presynaptic terminals with

a frequency range between 0.1 and 0.3 events per minute per ROI (Figure 2C), more than an order of magnitude lower than the expected frequency of spontaneous fusion events previously detected in single release sites (Leitz and Kavalali, 2014; Reese and Kavalali, 2015, 2016). Nevertheless, in all boutons, baclofen exerted some inhibition of baseline fluorescence intensity (Figure 2C), which is a reporter of resting Ca^{2+} signals. More prominently, baclofen reduced the frequency and amplitude of pmSCTs (Figure 2C), confirming the presence of a Ca^{2+} -dependent mode of inhibition, most likely through direct $\text{G}\beta\gamma$ inhibition of VGCCs in our experimental setting (De Waard et al., 1997; Herlitze et al., 1996; Holz et al., 1986). Due to the low frequency of pmSCTs per ROI, we also conducted imaging experiments in an 8-mM Ca^{2+} bath solution to augment event detection. With the 8-mM Ca^{2+} bath solution, there was an expected increase in baseline pmSCT frequency in addition to significant baclofen-induced inhibition, supporting the accuracy of our measurements at 2 mM Ca^{2+} (see Table S1).

Although baclofen-mediated inhibition of presynaptic spontaneous Ca^{2+} transients may partially account for GABA_B -receptor-mediated inhibition of spontaneous neurotransmitter release, spontaneous release does not depend on VGCCs to the same extent as the evoked release does. This premise is also supported by the data we presented above demonstrating that, in our system, spontaneous presynaptic Ca^{2+} transients occur at a lower frequency range than the actual spontaneous fusion events. Thus, a potential Ca^{2+} -independent mode of inhibition may play a greater role in inhibition of spontaneous release compared with its evoked counterpart. Even though the VGCC dependency of spontaneous release is still a matter of debate, recent studies suggest that spontaneous glutamate release partially depends on Ca^{2+} coming from sources other than VGCCs and uses $\text{Doc}2\alpha$ as Ca^{2+} sensor, whereas spontaneous GABA release partially depends on VGCC-mediated Ca^{2+} and uses both synaptotagmin 1 (Synt1) and $\text{Doc}2\beta$ as calcium sensors (see Figure 1B; Courtney et al., 2018; Goswami et al., 2012; Williams et al., 2012; Williams and Smith, 2018). Ten minutes incubation with 50 μM BAPTA-AM, an exogenous intracellular Ca^{2+} chelator with approximately 40-fold faster kinetics than EGTA-AM, was shown to inhibit VGCC-driven spontaneous GABA release (Williams et al., 2012). In contrast, EGTA-AM application was ineffective, suggesting that not the bulk intracellular Ca^{2+} but the Ca^{2+} influx from tightly coupled VGCCs drives spontaneous GABA release (Williams et al., 2012). Even though spontaneous glutamate release is now thought to be independent of VGCC-mediated Ca^{2+} influx, one notable study disagreed and showed that 20 μM BAPTA-AM, but not EGTA-AM, can occlude the inhibitory effects of a cocktail composed of inhibitors of P/Q, N, and R type VGCCs in 10–20 min (Ermolyuk et al., 2013). Considering the aforementioned data, we decided to preincubate with 100 μM BAPTA-AM for 20 min to suppress putative VGCC-driven spontaneous GABA release and glutamate release. Then, we recorded mEPSCs and mIPSCs in whole-cell voltage-clamp mode before and during 10 μM baclofen perfusion to investigate whether a Ca^{2+} -independent inhibitory mechanism distal to VGCCs operate for spontaneous glutamate and GABA release.

BAPTA-AM 20-min and 40-min preincubation resulted in a significant decrease in frequency of both mEPSCs (Figure 2D) and mIPSCs (Figure 2F) without any changes in amplitude, consistent with previous studies. Since BAPTA-AM decreased baseline mEPSC frequency to the same degree at both time points (Figure 2D), we only investigated GABA_B

receptor activation following 20-min preincubation to avoid non-specific deleterious effects of long-term calcium chelation. Nevertheless, baclofen was still able to decrease the frequency of mEPSCs (Figure 2E) and mIPSCs (Figure 2G) to the same degree in BAPTA-AM preincubated cultures, confirming the presence of a Ca^{2+} -independent mode of inhibition of spontaneous neurotransmitter release. We compared the percentage of baclofen-mediated inhibition between DMSO and BAPTA-AM preincubation to assess the relative contributions of Ca^{2+} -dependent and -independent modes of inhibition among the overall inhibition. Here, we found no differences for either mEPSCs (Figure 2E) or mIPSCs (Figure 2G). Taken together, the data we present so far strongly suggest that a Ca^{2+} -independent mechanism dominates the inhibition of spontaneous release by GABA_B receptor activation.

SNAP25 3 prevents baclofen-mediated inhibition of excitatory, but not inhibitory, spontaneous release

Possible locations of inhibition downstream of VGCCs are the Ca^{2+} sensors for neurotransmitter release and the actual release machinery that drives synaptic vesicle exocytosis. SNARE complex, composed of syb2 on the synaptic vesicle and syntaxin-1 and SNAP25 on the presynaptic terminal, is the canonical release machinery involved in both evoked and spontaneous release. Earlier experimental evidence suggests that $\text{G}\beta\gamma$ can directly bind to SNARE complex (Blackmer et al., 2005) and is responsible for the $\text{G}_{\text{I}/\text{O}}$ -mediated inhibition of evoked neurotransmitter release downstream of VGCCs. Biochemical studies mapped the C terminus end of the SNARE complex as the binding site for $\text{G}\beta\gamma$, as such botulinum-A-cleaved SNARE complexes have substantially reduced $\text{G}\beta\gamma$ binding (Blackmer et al., 2005). However, botulinum-A-cleaved SNARE complex is not able to sustain neurotransmitter release and thus is a poor tool to study synaptic physiology. Instead, previous studies utilized a truncated form of SNAP25, namely SNAP25 3, of which the last 3 amino acids from the C terminus are clipped off, can sustain evoked neurotransmitter release like wild-type (WT) SNAP25 but has significantly decreased $\text{G}\beta\gamma$ binding (Zurawski et al., 2016). A transgenic knockin mouse model harboring homozygous expression of SNAP25 3 was established using CRISPR-Cas9 system and was recently characterized (Zurawski et al., 2019).

Here, we prepared primary dissociated hippocampal cultures from homozygous SNAP25 3 mice or their WT littermates and recorded mEPSCs and mIPSCs at baseline and during baclofen perfusion. SNAP25 3 neurons had similar baseline mEPSC frequency and amplitude to that of WT SNAP25 (Figure 3A). Interestingly, SNAP25 3 completely prevented baclofen-induced decrease in mEPSC frequency (Figure 3B), suggesting that previously suggested Ca^{2+} -independent mode of inhibition of evoked release via $\text{G}\beta\gamma$ -SNARE interaction operates for spontaneous excitatory release as well. Since the spontaneous glutamate release is independent of VGCCs (Courtney et al., 2018; Williams and Smith, 2018), this mode of inhibition may be the primary mode of inhibition. Indeed, the lack of baclofen-induced inhibition of mEPSCs in SNAP25 3 suggests $\text{G}\beta\gamma$ -SNARE binding is the sole mode of inhibition of spontaneous glutamate release.

We also recorded mIPSCs to investigate the role of G $\beta\gamma$ -SNARE interaction in spontaneous GABA release. In contrast to mEPSCs, there was a decrease in baseline frequency of mIPSCs (Figure 3C), which is in parallel with our findings upon expression of myr ct-GRK2 (Figure 1J). Furthermore, a baclofen-induced reduction in mIPSC frequency was still present in SNAP25⁻³ neurons (Figure 3D). There were no changes in the amplitudes of mEPSCs or mIPSCs, excluding a postsynaptic effect of SNAP25⁻³ and baclofen (Figures 3A and 3C). To examine an alternative target of G $\beta\gamma$, we investigated the role of phospholipase C (PLC) downstream of G $\beta\gamma$ activation (Selbie and Hill, 1998). Following PLC inhibition, the percent decrease in mEPSC frequency upon baclofen treatment is more than 3-fold greater relative to the control group, with no difference in mIPSCs (see Table S1). This result may indicate that GABA_B receptor activation may concomitantly activate PLC, augmenting mEPSC frequency via several signaling pathways activated by PIP₂ hydrolysis, as well as cause direct inhibition of SNARE machinery. Therefore, PLC inhibition may unmask the true degree of inhibition achieved by direct G $\beta\gamma$ inhibition of SNARE machinery. Taken together with the data we presented above—regarding presynaptic Ca²⁺ transients and their limited impact on GABA_B-mediated inhibition on spontaneous release—these results suggest that baclofen may cause inhibition of mIPSCs through Ca²⁺-independent mechanisms utilizing alternate (non-SNAP25 or VGCC) targets of G $\beta\gamma$ subunits.

Synaptotagmin-1 modulates baclofen-induced inhibition of spontaneous glutamate release

Synaptotagmin-1 (Syt1) is the Ca²⁺ sensor for fast synchronous evoked release (Fernandez-Chacon et al., 2001). Experimental evidence suggests that it interacts with the SNARE complex through both Ca²⁺-independent stable interfaces (Zhou et al., 2015, 2017), as well as in a Ca²⁺-dependent manner through C terminus of SNAP25 (Zhang et al., 2002). Interestingly, G $\beta\gamma$ was shown to compete with Syt1 for the SNARE binding in a Ca²⁺-dependent manner (Blackmer et al., 2005; Yoon et al., 2007), as such increasing Ca²⁺ concentrations would allow a better Syt1 binding, thus displacing G $\beta\gamma$ from the SNARE complex (Yoon et al., 2007). The opposite is thought to be the mechanism of inhibition of evoked release with G $\beta\gamma$ binding to SNARE complex. In this case, G $\beta\gamma$ simply displaces Syt1 from SNARE complex and hence leads to uncoupling the local Ca²⁺ increase from the vesicular fusion. We used a high-efficiency, lentivirus-based delivery system to knock down Syt1 to investigate this phenomenon. With this approach, we were able to virtually knock out Syt1 with approximately 98% reduction in Syt1 protein levels (Figure 4A; Li et al., 2017). We used bipolar field stimulation and recorded evoked inhibitory postsynaptic currents (eIPSCs). With Syt1 knockdown (KD), the peak amplitudes of eIPSCs were reduced and asynchronous release became evident (Figure 4B). We monitored the normalized peak amplitudes over time by delivering stimulation every 10 s at baseline and during baclofen perfusion. Interestingly, at steady state during baclofen perfusion, Syt1 KD caused a more robust reduction of peak amplitudes (Figure 4B), suggesting that, apart from displacing Syt1, there is another layer of inhibition that becomes more pronounced upon attenuation of competition with Syt1.

As mentioned previously, spontaneous glutamate release does not utilize Syt1 as Ca²⁺ sensor; however, Syt1 clamps spontaneous release (Courtney et al., 2018). If there is another layer of inhibition (other than displacing Syt1 from SNARE complex) secondary to direct

Gβγ-SNARE binding, there should be a more robust inhibition of spontaneous glutamate release with baclofen, when Syt1 is knocked down. Moreover, in contrast to spontaneous GABA release, VGCCs are not involved and Syt1 does not drive mEPSCs, eliminating further confounders. Here, Syt1 KD resulted in unclamping of spontaneous release as evident by increased mEPSC frequency (Figure 4C). When perfused with baclofen, mEPSC frequencies decreased in both control and Syt1 KD (Figure 4D); however, the inhibition in Syt1 KD was more robust and almost doubled (Figure 4D). This is parallel with our previous observation of minor but significant increase of inhibition of eIPSCs with Syt1 KD, suggesting that displacing Syt1 from SNARE complex is not the only inhibitory effect of Gβγ-SNARE binding. Next, we repeated the same experiment while recording mIPSCs, representing spontaneous GABA release. Syt1 does not only clamp spontaneous GABA release but also drives it, making it harder to interpret changes associated with Syt1 KD. Nonetheless, Syt1 KD unclamped spontaneous GABA release (Figure 4E), baclofen reduced mIPSC frequencies for both control and Syt1 KD (Figure 4F), and the amount of inhibition was comparable (Figure 4F). Furthermore, we overexpressed Syt1 in our system to investigate whether we could occlude baclofen-mediated inhibition. Approximately 20% overexpression of Syt1 did not alter the degree of inhibition via Gβγ or baseline mEPSC spontaneous neurotransmission (see Table S1), suggesting a limited role of Syt1 competition in Gβγ inhibition or sufficiently high levels of endogenous Syt1 in the system that cannot be impacted in a functionally relevant manner via overexpression. However, we cannot exclude the possibility that undertrafficking of overexpressed Syt1 proteins to synaptic vesicles may also pose a limitation to occlude the baclofen-induced inhibition on mEPSC frequency. Taken together, these findings suggest that, while inhibition of mEPSCs operates via SNARE-Gβγ interaction modulated by Syt1, GABAergic spontaneous events are inhibited by Gβγ via alternative targets.

DISCUSSION

Studies in the last decade suggest that spontaneous release events function autonomously in regulation of synaptic plasticity and homeostasis (Andreae and Burrone, 2018; Gonzalez-Islas et al., 2018; Kavalali, 2015). In addition, recent evidence indicates that aberrant spontaneous release may underlie diverse clinical manifestations associated with developmental and epileptic encephalopathies of infancy and childhood (Alten et al., 2021) and spontaneous release process may form a substrate for rapid antidepressant action and other forms of neuropsychiatric treatments (Kavalali and Monteggia, 2012, 2020). Modulation of the different forms of neurotransmitter release in both directions through agonists, antagonists, and allosteric modulators of GPCRs is clinically beneficial in a wide variety of disorders (Benarroch, 2012; Bowery, 2006). Therefore, there is a critical need to better understand how spontaneous release is regulated by different modulators to develop therapeutics that can selectively inhibit evoked versus spontaneous neurotransmitter release.

GABA_B receptors are one of the most widely characterized G_{I/O}-coupled GPCRs, expressed widely in the mammalian nervous system, and respond to GABA, the main inhibitory neurotransmitter. Our data suggest that baclofen-triggered activation of GABA_B receptors leads to inhibition of spontaneous glutamate release primarily through Gβγ-SNARE interaction, whereas inhibition of spontaneous GABA release is also mediated by Gβγ

but may involve other targets, including a differential role for the Ca^{2+} sensor Syt1 in the regulation of the two forms of spontaneous release as well as possibly regulation of baseline diacylglycerol (DAG) or cAMP signaling (Maximov et al., 2007; Virmani et al., 2005). These findings are also in line with earlier evidence demonstrating that spontaneous glutamate release does not rely on VGCCs, whereas spontaneous GABA release does.

Our experiments showed that scavenging $\text{G}\beta\gamma$ by membrane-targeted myr ct-GRK2 was significantly effective in suppression of GABA_B -receptor-mediated inhibition of spontaneous release. Previous studies utilizing ct-GRK2 delivered purified ct-GRK2 peptides directly into the presynaptic terminal via microinjection and showed that ct-GRK2 fully occludes $\text{G}\beta\gamma$ -mediated inhibition of evoked release when paired pre- and postsynaptic recordings were performed (Blackmer et al., 2001). In contrast, we had to deliver ct-GRK2 using a lentiviral expression system in order to ensure that the majority of presynaptic terminals express the scavenger to investigate its effect on spontaneous release. This approach significantly differs from direct delivery by two means: (1) the delivery is rather chronic (over the course of days) compared with direct delivery, thus possibly leading to compensatory changes, and (2) the level of expression is inherently limited and likely does not reach similar levels to that of direct delivery. Nevertheless, expression of soluble ct-GRK2 showed a trend toward attenuation of baclofen-induced inhibition of spontaneous release, which became more robust and statistically significant upon myristoylation that anchors ct-GRK2 to the membrane. Therefore, our data, along with previously published data, suggest that $\text{G}\beta\gamma$ is the mediator for GABA_B -receptor-mediated inhibition of spontaneous release, and its location of action is the vicinity of plasma membrane, where VGCCs and docked and primed vesicles with SNARE complexes are located. It is important to note that, following expression of myr ct-GRK2 or in SNAP25 3 neurons, the baseline frequency of mIPSCs was decreased, whereas no changes were observed in baseline mEPSC frequencies. Interestingly, the direction of change (decreased frequency) was the opposite of what was expected (increased frequency secondary to elimination of the $\text{G}\beta\gamma$ -mediated inhibition). This suggests the presence of a dynamic and longer lasting regulation of spontaneous GABA release via GPCRs.

The $\text{G}\beta\gamma$ -mediated inhibition of Ca^{2+} influx through VGCCs is well characterized and largely accounts for the inhibition of action-potential-triggered evoked release, given that evoked release vitally depends on activation of presynaptic VGCCs. However, several studies showed that there is a parallel inhibition that is Ca^{2+} independent (Dittman and Regehr, 1996; Scanziani et al., 1992), which was later suggested to be direct $\text{G}\beta\gamma$ binding to SNARE complex (Blackmer et al., 2001, 2005). Unfortunately, our understanding of how SNARE complex mediates and at the same time clamps spontaneous synaptic vesicle exocytosis with different interaction partners, such as complexin and synaptotagmin-1, remains limited (Grushin et al., 2019; Ramakrishnan et al., 2020; Zhou et al., 2015, 2017). However, our study adds a facet to SNARE-mediated regulation of spontaneous fusion by providing evidence that, following receptor activation, $\text{G}\beta\gamma$ may act to suppress spontaneous fusion, thus adding a layer of inhibition in addition to displacement of Syt1 from the SNARE complex (see Figure 4 and related subsection). This premise is also consistent with the earlier finding that $\text{G}\beta\gamma$ binds to the C-terminal end of SNAP25 (Blackmer et al., 2005; Yoon et al., 2007), where the energy generated by the N-to-C-terminal zippering of the

SNARE complex is translated to the membrane fusion (Fang et al., 2008), and GABA_B receptor activation increases the energy barrier for vesicle fusion (Rost et al., 2011). It should be noted that a previous study showed an inhibitory effect of baclofen on release rescued with ionomycin after the cells were treated with botulinum A to cleave SNAP25 and concluded that C terminus SNAP25 cannot be the target for Ca²⁺-independent inhibition distal to VGCCs (Rost et al., 2011). However, Gβγ can also bind to the other SNAREs, such as syntaxin-1 (Blackmer et al., 2005; Yoon et al., 2007), and botulinum A application does not completely eliminate Gβγ binding to the SNARE complex composed of cleaved SNAP25, even though it markedly reduced it (Blackmer et al., 2005). Taken together, SNAP25⁻³ should be used merely as a tool while waiting for further structural studies to reveal Gβγ-SNARE interactions.

Overall, our data taken together with earlier studies suggest that GABA_B receptor activation inhibits spontaneous glutamate release via Gβγ-SNARE interaction, whereas inhibition of spontaneous GABA release also operates through Gβγ action via targets other than SNAP25 C-terminal. These results uncover a mechanism by which spontaneous neurotransmission, in particular action-potential-independent release of glutamate, can be selectively regulated independent of presynaptic Ca²⁺ signaling, suggesting a target for neurotherapeutic interventions.

Limitations of the study

While our data demonstrate Gβγ-mediated inhibition of spontaneous release in dissociated hippocampal cultures, a commonly used model in the field of synaptic physiology, the characteristics of spontaneous release in terms of rate, calcium dependence, utilized calcium sources, and involved SNAREs, may differ in other neuronal types. This limitation may also contribute to contradicting results from other groups with different models regarding the calcium dependence of spontaneous release. Furthermore, we were unable to identify a target for Gβγ-mediated inhibition of spontaneous GABA release, although we clearly showed spontaneous GABA release is modulated differently compared with spontaneous glutamate release. Although no changes were observed in spontaneous release frequency when GABA_B receptor antagonists were perfused to investigate the presence of potential Gβγ-mediated tonic inhibition in mature cultured neurons, baseline changes in mIPSC frequency following myr ct-GRK expression and in SNAP25⁻³ cultures indicated a role of tonic Gβγ-mediated inhibition during development, which was not further explored in this study. Finally, even though Gβγ-SNARE interactions were shown biochemically and functionally before and including this study, the field would greatly benefit from structural data to delineate the nature of the interactions and to better manipulate the system for further exploration.

STAR★METHODS

RESOURCE AVAILABILITY

Lead contact—Further information and requests for resources and reagents should be directed to and will be fulfilled by the lead contact, Ege T. Kavalali (ege.kavalali@vanderbilt.edu).

Materials availability—Myristoylated ct-GRK2 plasmid generated in this study have been deposited to Addgene (ID: 178734).

Data and code availability

- Full western blot images are presented within the figures. Microscopy data reported in this paper will be shared by the lead contact upon request.
- No original code has been generated for this study.
- Any additional information required to reanalyze the data reported in this paper is available from the lead contact upon request.

EXPERIMENTAL MODELS AND SUBJECT DETAILS

Animals—Postnatal day 2–3 Sprague-Dawley rats of either sex were used for the experiments described in Figures 1, 2, and 4. Pregnant Sprague-Dawley rats were housed individually until they give birth to a litter. The rats were kept in 12 hours : 12 hours dark:light cycle. The pregnant rats were provided with treats as well as cardboard enrichments. Postnatal day 2-3 littermates were used to prepare primary dissociated hippocampal cultures. SNAP25⁻³ (Zurawski et al., 2019) and WT SNAP25 littermate mice either sex were used for experiments described in Figure 3. They were provided with the same treats and the enrichments and kept in the same dark:light cycle as the previously described rats were subjected to. All animal procedures were performed in accordance with the guide for the care and use of laboratory animals and were approved by the Institutional Animal Care and Use Committee at Vanderbilt University. Health status of the live animals were periodically checked and confirmed by the veterinary staff of animal facilities of the Vanderbilt University.

Primary dissociated hippocampal cultures—Briefly, either hippocampi or cortical tissue were dissected in ice cold 20% fetal bovine serum (FBS) containing Hanks' balanced salt solution. Tissues were then washed and treated with 10 mg/ml trypsin and 0.5 mg/ml DNase at 37°C for 10 mins. The tissues were washed again, dissociated using filtered P1000 tip and centrifuged at 170g for 10 mins at 4°C. Pellet containing neurons was resuspended in plating medium containing MEM (no phenol red), 5 g/l D-glucose, 0.2 g/l NaHCO₃, 0.1 g/l transferrin, 10% FBS, 2 mM L-glutamine and 20 mg/l insulin. Neurons were plated onto 12 mm coverslips coated with 1:50 MEM:Matrigel solution. Cultures were kept in humidified incubators at 37°C and gassed with 95% air and 5% CO₂. On DIV (day *in vitro*) 1, the plating medium replaced with 4 μM cytosine arabinoside containing growth medium. Growth medium is similar to plating medium except for the following: 5% FBS, 0.5 mM L-glutamine, no insulin and supplemented with B27 supplement. On DIV4, the cytosine arabinoside concentration was dropped 2 μM by performing a half media change and lentivirus containing supernatant was added to either express ct-GRK2/myr ct-GRK2 or knock down Syt1. Cultures were kept without any disruption until DIV14. All experiments were performed between DIV14-18, when synapses reached maturity and overexpression of the target protein was plateaued (Alten et al., 2021). Sample size was not predetermined using statistical methods prior to experimentation. Sample sizes were based on previous studies in the field of molecular & cellular neuroscience.

Cell lines—Human embryonic kidney-293 (HEK293) cells (ATCC) were used to produce lentiviral particles to infect primary neuronal cultures. HEK293 cultures were kept in humidified incubators at 37°C and gassed with 95% air and 5% CO₂. The cells were split and passaged when they reached 80% confluency. The culture medium consisted of 10% FBS containing Dulbecco's Modified Eagle Medium supplemented with penicillin and streptavidin.

In vitro studies—NEB Turbo Competent E. coli (NEB) were used for standard molecular cloning methods.

METHOD DETAILS

Cloning and lentivirus preparation—ct-GRK2 and myr ct-GRK2 were cloned into pFUGW expression vector containing human ubiquitin promoter using standard molecular biology methods and verified by sequencing. Empty pFUGW backbone was used as a control in functional experiments. HEK293 cells were cotransfected by pFUGW and three packaging plasmids (pCMV-VSV-G (Stewart et al., 2003), pMDLg/pRRE (Dull et al., 1998), pRSV-Rev (Dull et al., 1998) using FuGENE 6 transfection reagent (Promega). 24 hours after the transfection, HEK cell media containing the transfection cocktail was replaced by neuronal growth medium. 48 hours after the media change, the media containing lentiviral particles was collected and centrifuged at 2500 rpm for 15 mins at 4°C to get rid of debris. 200 µl of supernatant was directly added to cultures DIV4 to infect the neurons.

Electrophysiology and data analysis—Whole-cell patch clamp recordings were performed on pyramidal cells using CV203BU headstage, Axopatch 200B amplifier, Digidata 1320 digitizer and 8 Clampex 8.0 software (Molecular Devices). Recordings were filtered at 1 kHz and sampled at 100 µs. Experiments were conducted at room temperature. For external bath solution, a modified Tyrode's solution containing the followings was used: (in mM): 150 NaCl, 4 KCl, 1.25 MgCl₂, 2 CaCl₂, 10 D-glucose, 10 HEPES at pH 7.4. To isolate mEPSCs, 1 µM TTX, 50 µM PTX, and 50 µM D-AP5 were added. To isolate mIPSCs, 1 µM TTX, 10 µM CNQX, and 50 µM D-AP5 were added. To isolate eIPSCs, 50 µM D-AP5 and 10 µM CNQX were added. For eIPSC recordings, the field stimulation was provided using a parallel bipolar electrode (FHC) immersed in the external bath solution, delivering 35 mA pulses via a stimulus isolation unit. Throughout the evoked experiments where stimulations are delivered via a bipolar electrode, we used a programmable motorized Sutter micromanipulator to make sure that the location of the bipolar electrode is exactly the same in all experiments, so that a similar field of coverslip is stimulated each time. For BAPTA-AM experiments, coverslips were incubated either in 100 µM BAPTA-AM in 0.1% DMSO containing external bath solution with 0 mM Ca²⁺ or in vehicle for 20- or 40-minutes. For voltage clamp experiments, the membrane potential was held at -70 mV and the 3-5 MΩ borosilicate glass patch pipettes were filled with the internal solution contained the following (in mM): 115 Cs-MeSO₃, 10 CsCl, 5 NaCl, 10 HEPES, 0.6 EGTA, 20 tetraethylammonium-Cl, 4 Mg-ATP, 0.3 Na₃GTP, and 10 QX-314 [N-(2,6-dimethylphenylcarbamoylmethyl)-triethylammonium bromide] at pH 7.35 and 300 mOsm. For all recordings included for the analysis, the membrane resistance was greater than 100 MΩ, the access resistance was less than 20 MΩ and time constant (τ) was less

than 3 ms. mPSC frequencies and amplitudes were analyzed using Mini Analysis software (Synaptosoft). Evoked IPSCs were analyzed by using Clampfit (Molecular Devices).

Live imaging and data analysis—DIV 18-20 cultured hippocampal neurons expressing syb2-GCaMP6s were used in imaging experiments. The external bath solution of modified Tyrode's (as described above) was used with TTX, AP-5 and PTX. For 8mM Ca²⁺ experiments Tyrode's bath solution Ca²⁺ concentration was increased with appropriate adjustments to account for osmolarity. Experiments were performed at room temperature using an EMCCD camera, collected on a Nikon Eclipse TE2000-U microscope with a 60X Plan Apo objective (Nikon). For illumination, a Lambda-DG4 (Sutter instruments) with a GFP filter was used. Images were acquired at an acquisition rate of 10 Hz with no binning. Fluorescence intensity was recorded for 5 minutes at baseline and for 5 minutes following the perfusion of Tyrode's solution containing 10 μM baclofen (for 8mM Ca²⁺ experiments each treatment group was recorded for 5 minutes). At the end of the experiment 90 mM KCL was perfused for the selection of regions of interest (ROIs) for analysis. Following image acquisition, fluorescence intensity analysis was performed using a custom-made macro for FIJI to automatically select ROIs. The fluorescence intensity of ROIs were analyzed using a Matlab (Mathworks) script, based on our previous imaging analysis (Li et al., 2017; Chanaday and Kavalali, 2018). The script was used to detect and analyze fluorescent peaks representing presynaptic miniature spontaneous Ca²⁺ transients (pmSCTs) in synaptic ROIs.

Protein quantification—To quantify protein levels, western blotting was carried out. Briefly, protein samples were prepared from coverslips using Laemmli Buffer containing protease and phosphatase inhibitor cocktails (Roche) and beta-mercaptoethanol. Samples were sonicated and/or boiled and loaded on SDS-PAGE gels and transferred to nitrocellulose membranes. Membranes were incubated with primary antibodies at 4°C overnight in following dilutions: 1:10000 Anti-GAPDH rabbit (14C10, Cell Signaling), 1:1000 Anti-synaptotagmin-1 mouse (105-011, Synaptic Systems) and 1:2000 Anti-GRK2 rabbit (ab137666, Abcam). After incubation with fluorescent secondary anti-rabbit and anti-mouse antibodies (IRDye Secondary Antibodies, Licor), membranes were imaged using an Odyssey CLx imaging system (Licor). Band intensities were analyzed using ImageJ and normalized to loading controls.

QUANTIFICATION AND STATISTICAL ANALYSIS

The data was presented as mean ± standard error of mean, unless stated otherwise in the figure legends. The sample size for each experiment was shown in the figure and was not predetermined using statistical methods prior to experimentation. For patch-clamp electrophysiology experiments, the sample size corresponds to number of cells patched. Sample sizes were based on previous studies in the field of molecular & cellular neuroscience. Each set of experiments was performed twice with two different sets of neuronal cultures if appropriate to confirm the results. Prism 8 (Graphpad) was used to run statistical tests. Outliers were identified with Robust regression and Outlier removal (ROUT) method. Tests ran for each set of experiments were stated in the figure legends. Statistical information for each figure is stated in Table S1. More detail on Figure 4B

analysis: to statistically assess the effect of Syt1 KD the mean values of eIPSC amplitudes were horizontally fitted, and fits were compared for the data at steady state (ctrl: $y = 0.6049$, Syt KD $y = 0.5141$). The null hypothesis of the sum of squares F-test is one curve can be fitted for both the WT and Syt1 KD groups, this was rejected, demonstrating a significant difference between the two groups. p value less than 0.05 was considered as statistically significant. Significance levels are stated as follows: * $p < 0.05$, ** $p < 0.01$, *** $p < 0.001$ and **** $p < 0.0001$. ns denotes non-significance.

Supplementary Material

Refer to Web version on PubMed Central for supplementary material.

ACKNOWLEDGMENTS

We thank Brent A. Trauterman and Analisa D. Thompson Gray for their assistance. The mCherry-Syt1 short hairpin RNA (shRNA) knockdown construct was a generous gift from Dr. Thomas Südhof. This research was supported by R01MH66198 and R01AG055577 to E.T.K. and 1R01EY10291, 1R01DK109204, and 1R01NS111749 to H.E.H from the National Institutes of Health. Figures 1A, 1B, 1C, and 1F were created with BioRender.com.

REFERENCES

- Alten B, Zhou Q, Shin OH, Esquivies L, Lin PY, White KI, Sun R, Chung WK, Monteggia LM, Brunger AT, and Kavalali ET (2021). Role of aberrant spontaneous neurotransmission in SNAP25-associated encephalopathies. *Neuron* 109, 59–72 e55. [PubMed: 33147442]
- Andreae LC, and Burrone J (2018). The role of spontaneous neurotransmission in synapse and circuit development. *J. Neurosci. Res* 96, 354–359. [PubMed: 29034487]
- Bean BP (1989). Neurotransmitter inhibition of neuronal calcium currents by changes in channel voltage dependence. *Nature* 340, 153–156. [PubMed: 2567963]
- Benarroch EE (2012). GABAB receptors: structure, functions, and clinical implications. *Neurology* 78, 578–584. [PubMed: 22351795]
- Blackmer T, Larsen EC, Bartleson C, Kowalchuk JA, Yoon EJ, Preininger AM, Alford S, Hamm HE, and Martin TF (2005). G protein betagamma directly regulates SNARE protein fusion machinery for secretory granule exocytosis. *Nat. Neurosci* 8, 421–425. [PubMed: 15778713]
- Blackmer T, Larsen EC, Takahashi M, Martin TF, Alford S, and Hamm HE (2001). G protein betagamma subunit-mediated presynaptic inhibition: regulation of exocytotic fusion downstream of Ca^{2+} entry. *Science* 292, 293–297. [PubMed: 11303105]
- Bowery NG (2006). GABAB receptor: a site of therapeutic benefit. *Curr. Opin. Pharmacol* 6, 37–43. [PubMed: 16361115]
- Chanaday NL, and Kavalali ET (2018). Optical detection of three modes of endocytosis at hippocampal synapses. *eLife* 7, e36097. [PubMed: 29683423]
- Chanaday NL, Nosyreva E, Shin OH, Zhang H, Aklan I, Atasoy D, Bezprozvanny I, and Kavalali ET (2021). Presynaptic store-operated Ca^{2+} entry drives excitatory spontaneous neurotransmission and augments endoplasmic reticulum stress. *Neuron* 109, 1314–1332.e5. [PubMed: 33711258]
- Courtney NA, Briguglio JS, Bradberry MM, Greer C, and Chapman ER (2018). Excitatory and inhibitory neurons utilize different Ca^{2+} sensors and sources to regulate spontaneous release. *Neuron* 98, 977–991 e975. [PubMed: 29754754]
- De Waard M, Liu H, Walker D, Scott VE, Gurnett CA, and Campbell KP (1997). Direct binding of G-protein betagamma complex to voltage-dependent calcium channels. *Nature* 385, 446–450. [PubMed: 9009193]
- Dittman JS, and Regehr WG (1996). Contributions of calcium-dependent and calcium-independent mechanisms to presynaptic inhibition at a cerebellar synapse. *J. Neurosci* 16, 1623–1633. [PubMed: 8774431]

- Dull T, Zufferey R, Kelly M, Mandel RJ, Nguyen M, Trono D, and Naldini L (1998). A third-generation lentivirus vector with a conditional packaging system. *J. Virol* 72, 8463–8471. [PubMed: 9765382]
- Dunlap K, and Fischbach GD (1978). Neurotransmitters decrease the calcium component of sensory neurone action potentials. *Nature* 276, 837–839. [PubMed: 31570]
- Ermolyuk YS, Alder FG, Surges R, Pavlov IY, Timofeeva Y, Kullmann DM, and Volynski KE (2013). Differential triggering of spontaneous glutamate release by P/Q-, N- and R-type Ca²⁺ channels. *Nat. Neurosci* 16, 1754–1763. [PubMed: 24185424]
- Fang Q, Berberian K, Gong LW, Hafez I, Sorensen JB, and Lindau M (2008). The role of the C terminus of the SNARE protein SNAP-25 in fusion pore opening and a model for fusion pore mechanics. *Proc. Natl. Acad. Sci. U S A* 105, 15388–15392. [PubMed: 18829435]
- Fernandez-Chacon R, Konigstorfer A, Gerber SH, Garcia J, Matos MF, Stevens CF, Brose N, Rizo J, Rosenmund C, and Sudhof TC (2001). Synaptotagmin I functions as a calcium regulator of release probability. *Nature* 410, 41–49. [PubMed: 11242035]
- Frangaj A, and Fan QR (2018). Structural biology of GABAB receptor. *Neuropharmacology* 136, 68–79. [PubMed: 29031577]
- Gonzalez-Islas C, Bulow P, and Wenner P (2018). Regulation of synaptic scaling by action potential-independent miniature neurotransmission. *J. Neurosci. Res* 96, 348–353. [PubMed: 28782263]
- Goswami SP, Bucurenciu I, and Jonas P (2012). Miniature IPSCs in hippocampal granule cells are triggered by voltage-gated Ca²⁺ channels via microdomain coupling. *J. Neurosci* 32, 14294–14304. [PubMed: 23055500]
- Grushin K, Wang J, Coleman J, Rothman JE, Sindelar CV, and Krishnakumar SS (2019). Structural basis for the clamping and Ca(2+) activation of SNARE-mediated fusion by synaptotagmin. *Nat. Commun* 10, 2413. [PubMed: 31160571]
- Herlitze S, Garcia DE, Mackie K, Hille B, Scheuer T, and Catterall WA (1996). Modulation of Ca²⁺ channels by G-protein beta gamma subunits. *Nature* 380, 258–262. [PubMed: 8637576]
- Holz G.G.t., Rane SG, and Dunlap K (1986). GTP-binding proteins mediate transmitter inhibition of voltage-dependent calcium channels. *Nature* 319, 670–672. [PubMed: 2419757]
- Ikeda SR (1996). Voltage-dependent modulation of N-type calcium channels by G-protein beta gamma subunits. *Nature* 380, 255–258. [PubMed: 8637575]
- Kavalali ET (2015). The mechanisms and functions of spontaneous neurotransmitter release. *Nat. Rev. Neurosci* 16, 5–16. [PubMed: 25524119]
- Kavalali ET, and Monteggia LM (2012). Synaptic mechanisms underlying rapid antidepressant action of ketamine. *Am. J. Psychiatry* 169, 1150–1156. [PubMed: 23534055]
- Kavalali ET, and Monteggia LM (2020). Targeting homeostatic synaptic plasticity for treatment of mood disorders. *Neuron* 106, 715–726. [PubMed: 32497508]
- Leitz J, and Kavalali ET (2014). Fast retrieval and autonomous regulation of single spontaneously recycling synaptic vesicles. *Elife* 3, e03658. [PubMed: 25415052]
- Li YC, Chanaday NL, Xu W, and Kavalali ET (2017). Synaptotagmin-1- and synaptotagmin-7-dependent fusion mechanisms target synaptic vesicles to kinetically distinct endocytic pathways. *Neuron* 93, 616–631 e3. [PubMed: 28111077]
- Lipscombe D, Kongsamut S, and Tsien RW (1989). Alpha-adrenergic inhibition of sympathetic neurotransmitter release mediated by modulation of N-type calcium-channel gating. *Nature* 340, 639–642. [PubMed: 2570354]
- Luscher C, and Slesinger PA (2010). Emerging roles for G protein-gated inwardly rectifying potassium (GIRK) channels in health and disease. *Nat. Rev. Neurosci* 11, 301–315. [PubMed: 20389305]
- Maximov A, Shin OH, Liu X, and Sudhof TC (2007). Synaptotagmin-12, a synaptic vesicle phosphoprotein that modulates spontaneous neurotransmitter release. *J. Cell Biol* 176, 113–124. [PubMed: 17190793]
- Ramakrishnan S, Bera M, Coleman J, Rothman JE, and Krishnakumar SS (2020). Synergistic roles of Synaptotagmin-1 and complexin in calcium-regulated neuronal exocytosis. *Elife* 9.
- Reese AL, and Kavalali ET (2015). Spontaneous neurotransmission signals through store-driven Ca(2+) transients to maintain synaptic homeostasis. *Elife* 4.

- Reese AL, and Kavalali ET (2016). Single synapse evaluation of the postsynaptic NMDA receptors targeted by evoked and spontaneous neurotransmission. *Elife* 5.
- Rishal I, Porozov Y, Yakubovich D, Varon D, and Dascal N (2005). Gbetagamma-dependent and Gbetagamma-independent basal activity of G protein-activated K⁺ channels. *J. Biol. Chem* 280, 16685–16694. [PubMed: 15728579]
- Rost BR, Nicholson P, Ahnert-Hilger G, Rummel A, Rosenmund C, Breustedt J, and Schmitz D (2011). Activation of metabotropic GABA receptors increases the energy barrier for vesicle fusion. *J. Cell Sci* 124, 3066–3073. [PubMed: 21852427]
- Scanziani M, Capogna M, Gähwiler BH, and Thompson SM (1992). Presynaptic inhibition of miniature excitatory synaptic currents by baclofen and adenosine in the hippocampus. *Neuron* 9, 919–927. [PubMed: 1358131]
- Selbie LA, and Hill SJ (1998). G-protein-coupled-receptor cross-talk: the fine-tuning of multiple receptor-signalling pathways. *Trends Pharmacol. Sci* 19, 87–93. [PubMed: 9584624]
- Stewart SA, Dykxhoorn DM, Palliser D, Mizuno H, Yu EY, An DS, Sabatini DM, Chen IS, Hahn WC, Sharp PA, et al. (2003). Lentivirus-delivered stable gene silencing by RNAi in primary cells. *RNA* 9, 493–501. [PubMed: 12649500]
- Takahashi T, Kajikawa Y, and Tsujimoto T (1998). G-Protein-coupled modulation of presynaptic calcium currents and transmitter release by a GABAB receptor. *J. Neurosci* 18, 3138–3146. [PubMed: 9547222]
- Tedford HW, and Zamponi GW (2006). Direct G protein modulation of Cav2 calcium channels. *Pharmacol. Rev* 58, 837–862. [PubMed: 17132857]
- Virmani T, Ertunc M, Sara Y, Mozhayeva M, and Kavalali ET (2005). Phorbol esters target the activity-dependent recycling pool and spare spontaneous vesicle recycling. *J. Neurosci* 25, 10922–10929. [PubMed: 16306405]
- White JH, Wise A, Main MJ, Green A, Fraser NJ, Disney GH, Barnes AA, Emson P, Foord SM, and Marshall FH (1998). Heterodimerization is required for the formation of a functional GABA(B) receptor. *Nature* 396, 679–682. [PubMed: 9872316]
- Williams C, Chen W, Lee CH, Yaeger D, Vyleta NP, and Smith SM (2012). Coactivation of multiple tightly coupled calcium channels triggers spontaneous release of GABA. *Nat. Neurosci* 15, 1195–1197. [PubMed: 22842148]
- Williams CL, and Smith SM (2018). Calcium dependence of spontaneous neurotransmitter release. *J. Neurosci. Res* 96, 335–347. [PubMed: 28699241]
- Yoon EJ, Gerachshenko T, Spiegelberg BD, Alford S, and Hamm HE (2007). Gbetagamma interferes with Ca²⁺-dependent binding of synaptotagmin to the soluble N-ethylmaleimide-sensitive factor attachment protein receptor (SNARE) complex. *Mol. Pharmacol* 72, 1210–1219. [PubMed: 17715396]
- Zhang X, Kim-Miller MJ, Fukuda M, Kowalchuk JA, and Martin TF (2002). Ca²⁺-dependent synaptotagmin binding to SNAP-25 is essential for Ca²⁺-triggered exocytosis. *Neuron* 34, 599–611. [PubMed: 12062043]
- Zhou Q, Lai Y, Bacaj T, Zhao M, Lyubimov AY, Uervirojnangkoorn M, Zeldin OB, Brewster AS, Sauter NK, Cohen AE, et al. (2015). Architecture of the synaptotagmin-SNARE machinery for neuronal exocytosis. *Nature* 525, 62–67. [PubMed: 26280336]
- Zhou Q, Zhou P, Wang AL, Wu D, Zhao M, Sudhof TC, and Brunger AT (2017). The primed SNARE-complexin-synaptotagmin complex for neuronal exocytosis. *Nature* 548, 420–425. [PubMed: 28813412]
- Zurawski Z, Rodriguez S, Hyde K, Alford S, and Hamm HE (2016). Gbetagamma binds to the extreme C terminus of SNAP25 to mediate the action of Gi/o-coupled G protein-coupled receptors. *Mol. Pharmacol* 89, 75–83. [PubMed: 26519224]
- Zurawski Z, Thompson Gray AD, Brady LJ, Page B, Church E, Harris NA, Dohn MR, Yim YY, Hyde K, Mortlock DP, et al. (2019). Disabling the Gbetagamma-SNARE interaction disrupts GPCR-mediated presynaptic inhibition, leading to physiological and behavioral phenotypes. *Sci. Signal* 12, eaat8595. [PubMed: 30783011]

Highlights

- Scavenging $G\beta\gamma$ prevents $GABA_B$ -mediated inhibition of spontaneous release
- Regulation of spontaneous glutamate release involves $G\beta\gamma$ -SNARE interactions
- Synaptotagmin-1 modulates $G\beta\gamma$ -SNARE interactions for spontaneous glutamate release
- Regulation of spontaneous GABA release utilizes $G\beta\gamma$ through alternative targets

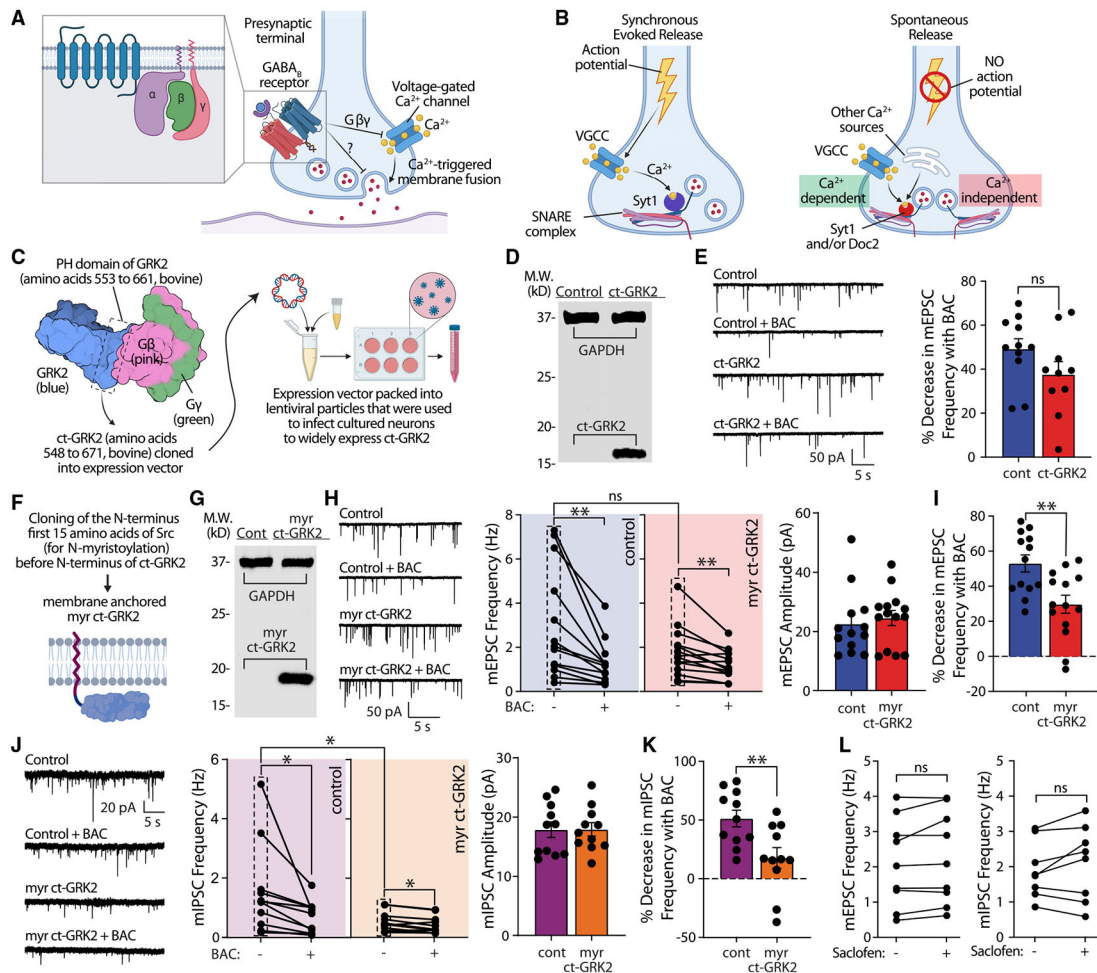


Figure 1. Scavenging Gβγ attenuates GABA_B-receptor-mediated inhibition of spontaneous release

(A) G-protein-coupled GABA_B receptor activation inhibits neurotransmitter release by inhibiting voltage-gated Ca²⁺-channel-mediated Ca²⁺ influx and/or by Ca²⁺-independent mechanisms, denoted with “?”.

(B) Fast synchronous evoked neurotransmitter release depends on opening of voltage-gated Ca²⁺ channels (VGCCs) triggered by an invading action potential at the presynaptic terminal. Local increase in Ca²⁺ concentration is sensed by synaptotagmin-1 (Syt1) and results in SNARE-complex-driven membrane fusion. On the other hand, spontaneous release does not require action potentials and is mediated by both Ca²⁺-dependent and -independent mechanisms. See the text for a detailed explanation of most recent experimental evidence on Ca²⁺ dependence of spontaneous release.

(C) Structure of GRK2-bound Gβγ (PDB: 1OMW) along with description of the experimental design. GRK2 is shown in blue, Gβ is shown in pink, and Gγ is shown in green.

(D) Immunoblot of protein samples obtained from control group (infected by lentiviral particles carrying empty backbone) and ct-GRK2 group (infected by lentiviral particles carrying ct-GRK expression vector).

(E) Representative traces of miniature excitatory postsynaptic currents (mEPSCs) recorded at baseline and during 10 μ M baclofen (BAC) perfusion along with quantitative analysis of % decrease in event frequency upon BAC perfusion compared with baseline (two-tailed, non-paired t test; control n = 11; ct-GRK2 n = 10).

(F) Description of manipulation of ct-GRK2 to obtain myristoylated ct-GRK2 (myr ct-GRK2).

(G) Immunoblot of protein samples obtained from control group (infected by lentiviral particles carrying empty backbone) and myr ct-GRK2 group (infected by lentiviral particles carrying myr ct-GRK expression vector). Compare with (E) and note the higher molecular weight of myr ct-GRK.

(H) Representative traces of mEPSCs recorded at baseline and during 10 μ M BAC perfusion along with quantitative analysis of event frequencies at baseline and during BAC perfusion. mEPSC frequencies at baseline and during BAC perfusion were compared using a two-tailed, paired t test, whereas mEPSC frequencies and amplitudes at baseline for control and myr ct-GRK2 were compared using a two-tailed, non-paired t test (control n = 13; myr ct-GRK2 n = 14).

(I) Percent decrease in mEPSC frequency upon BAC perfusion compared with baseline (two-tailed, non-paired t test; control n = 13; myr ct-GRK2 n = 14).

(J) Representative traces of miniature inhibitory postsynaptic currents (mIPSCs) recorded at baseline and during 10 μ M BAC perfusion along with quantitative analysis of event frequencies at baseline and during BAC perfusion. mIPSC frequencies at baseline and during BAC perfusion were compared using a two-tailed, paired t test, whereas mIPSC frequencies and amplitudes at baseline for control and myr ct-GRK2 were compared using a two-tailed, non-paired t test (control n = 11; myr ct-GRK2 n = 11).

(K) Percent decrease in mIPSC frequency upon BAC perfusion compared with baseline (two-tailed, non-paired t test; control n = 11; myr ct-GRK2 n = 11).

(L) Quantitative analyses of mEPSC and mIPSC frequencies at baseline and during GABA_B-receptor antagonist saclofen (200 μ M) perfusion (two-tailed, paired t test; mEPSC frequency n = 9; mIPSC frequency n = 8).

All panels: significance levels are stated as follows: *p < 0.05; **p < 0.01; ***p < 0.001; and ****p < 0.0001. ns denotes non-significance.

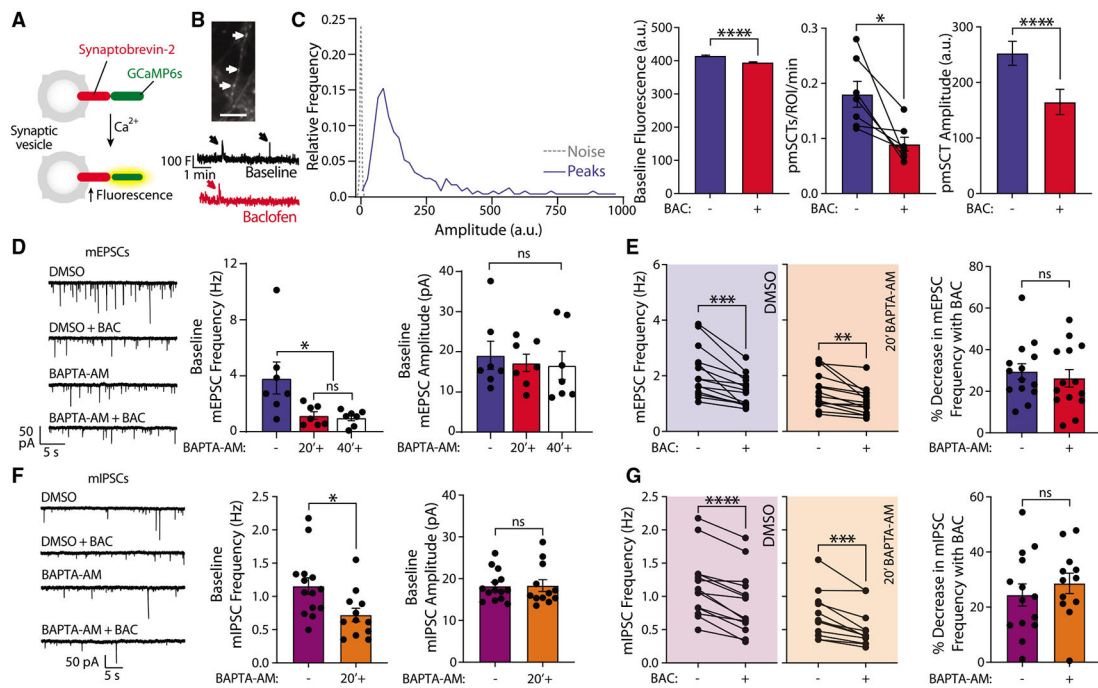


Figure 2. Baclofen can inhibit spontaneous release in a Ca^{2+} -dependent and -independent manner

(A) Illustration of synaptobrevin-2-attached calcium sensor GCaMP6s and its localization on the synaptic vesicles.

(B) Representative image from syb2-GCaMP6s expressing primary dissociated hippocampal cultures. Arrows denote a few examples of synaptic region of interests (ROIs). Scale bar corresponds to 10 μm . Representative raw traces were obtained from quantification of signals from individual ROIs.

(C) Quantitative analyses of frequency distribution of noise and presynaptic miniature spontaneous Ca^{2+} transient (pmSCT) amplitudes (peaks), baseline fluorescence signal (Wilcoxon; $n = 2,932$; n is ROI), number of pmSCTs per ROI per min (Wilcoxon; $n = 7$; n is coverslip), and pmSCT amplitude (Mann-Whitney U; baseline $n = 155$; BAC $n = 74$; n is peaks).

(D) Representative traces of mEPSCs recorded at baseline and during 10 μM BAC perfusion along with quantitative analysis of event frequencies and amplitudes at baseline for DMSO control and BAPTA-AM 20 and 40 min preincubation (one-way ANOVA; DMSO control $n = 7$; BAPTA-AM 20' $n = 7$; BAPTA-AM 40' $n = 7$).

(E) Quantitative analyses of mEPSC frequencies at baseline and during 10 μM BAC perfusion for DMSO control and BAPTA-AM 20-min preincubation (two-tailed, paired t test; DMSO $n = 14$; BAPTA-AM 20' $n = 14$), along with % decrease in mEPSC frequency upon BAC perfusion (two-tailed, non-paired t test; DMSO $n = 14$; BAPTA-AM 20' $n = 14$).

(F) Representative traces of mIPSCs recorded at baseline and during 10 μM BAC perfusion along with quantitative analysis of event frequencies and amplitudes at baseline for DMSO control and BAPTA-AM 20-min preincubation (two-tailed, non-paired t test; DMSO control $n = 14$; BAPTA-AM 20' $n = 12$).

(G) Quantitative analyses of mIPSC frequencies at baseline and during 10 μ M BAC perfusion for DMSO control and BAPTA-AM 20-min preincubation (two-tailed, paired t test; DMSO n = 14; BAPTA-AM 20' n = 12), along with % decrease in mIPSC frequency upon BAC perfusion (two-tailed, non-paired t test; DMSO n = 14; BAPTA-AM 20' n = 12). All panels: significance levels are stated as follows: *p < 0.05; **p < 0.01; ***p < 0.001; and ****p < 0.0001.

Author Manuscript

Author Manuscript

Author Manuscript

Author Manuscript

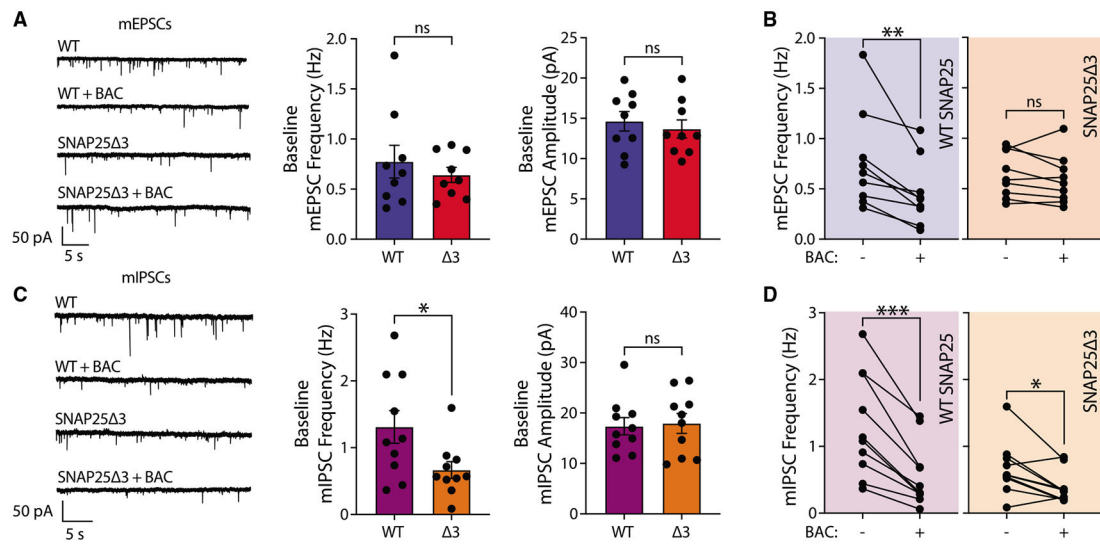


Figure 3. SNAP25 Δ 3 prevents baclofen-mediated inhibition of excitatory, but not inhibitory, spontaneous release

(A) Representative traces of mEPSCs recorded at baseline and during 10 μ M BAC perfusion along with quantitative analysis of event frequencies and amplitudes at baseline for WT SNAP25 control and SNAP25 Δ 3 (two-tailed, non-paired t test; WT n = 9; Δ 3 n = 9).

(B) Quantitative analyses of mEPSC frequencies at baseline and during 10 μ M BAC perfusion for WT SNAP25 control and SNAP25 Δ 3 (two-tailed, paired t test; WT n = 9; Δ 3 n = 9).

(C) Representative traces of mIPSCs recorded at baseline and during 10 μ M BAC perfusion along with quantitative analysis of event frequencies and amplitudes at baseline for WT SNAP25 control and SNAP25 Δ 3 (two-tailed, non-paired t test; WT n = 10; Δ 3 n = 10).

(D) Quantitative analyses of mIPSC frequencies at baseline and during 10 μ M BAC perfusion for WT SNAP25 control and SNAP25 Δ 3 (two-tailed, paired t test; WT n = 10; Δ 3 n = 10).

All panels: significance levels are stated as follows: *p < 0.05; **p < 0.01; ***p < 0.001; and ****p < 0.0001.

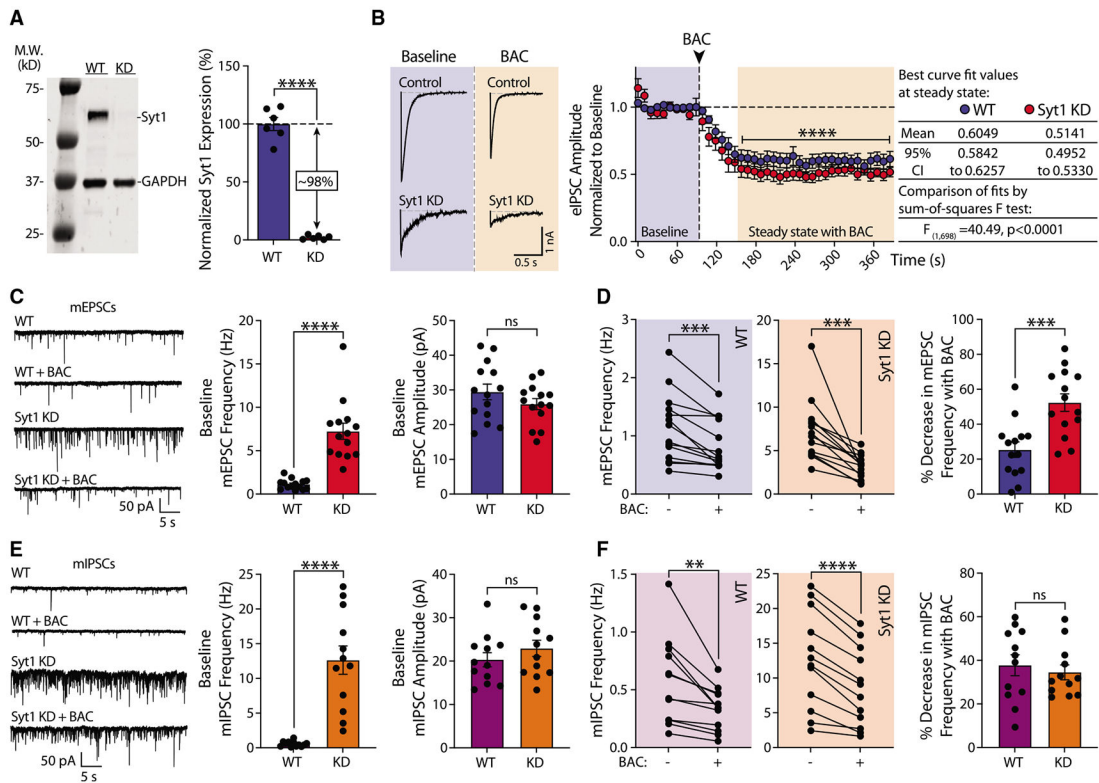


Figure 4. Synaptotagmin-1 modulates baclofen-induced inhibition of spontaneous glutamate release

(A) Representative immunoblot of protein samples obtained from control group (infected by lentiviral particles carrying empty backbone) and Syt1 KD group (infected by lentiviral particles carrying Syt1 shRNA construct) and its quantification (two-tailed, non-paired t test; WT n = 6; Syt1 KD n = 6).

(B) Representative evoked inhibitory postsynaptic currents (eIPSCs) elicited by single stimulus at baseline and during 10 μ M BAC perfusion. Note that the eIPSCs became smaller in amplitude and grossly asynchronous when Syt1 was knocked down (Syt1 KD). The effect of BAC on eIPSC amplitudes was quantified over time and normalized to baseline. At steady state, the mean values were horizontally fitted and fits were compared (WT n = 14; Syt1 KD n = 14).

(C) Representative traces of mEPSCs recorded at baseline and during 10 μ M BAC perfusion along with quantitative analysis of event frequencies and amplitudes at baseline for WT control and Syt1 KD (two-tailed, non-paired t test; WT n = 14; Syt1 KD n = 14).

(D) Quantitative analyses of mEPSC frequencies at baseline and during 10 μ M BAC perfusion for WT control and Syt1 KD (two-tailed, paired t test; WT n = 14; Syt1 KD n = 14), along with % decrease in mEPSC frequency upon BAC perfusion (two-tailed, non-paired t test; WT n = 14; Syt1 KD n = 14).

(E) Representative traces of mIPSCs recorded at baseline and during 10 μ M BAC perfusion along with quantitative analysis of event frequencies and amplitudes at baseline for WT control and Syt1 KD (two-tailed, non-paired t test; WT n = 12; Syt1 KD n = 12).

(F) Quantitative analyses of mIPSC frequencies at baseline and during 10 μ M BAC perfusion for WT control and Syt1 KD (two-tailed, paired t test; WT n = 12; Syt1 KD n = 12).

n = 12), along with % decrease in mIPSC frequency upon BAC perfusion (two-tailed, non-paired t test; WT n = 12; Syt1 KD n = 12).

All panels: significance levels are stated as follows: *p < 0.05; **p < 0.01; ***p < 0.001; and ****p < 0.0001.

Author Manuscript

Author Manuscript

Author Manuscript

Author Manuscript

KEY RESOURCES TABLE

REAGENT or RESOURCE	SOURCE	IDENTIFIER
Antibodies		
Anti-GAPDH (rabbit)	Cell signaling	Catalog # 14C10 RRID:AB_561053
Anti-synaptotagmin-1 (mouse)	Synaptic Systems	Catalog # 105-011 RRID:AB_887832
Anti-GRK2 C-terminal (rabbit)	Abcam	Catalog # ab137666 RRID: not available
Bacterial and virus strains		
NEB Turbo Competent <i>E. coli</i>	NEB	Catalog # C2984H
Chemicals, Peptides, and Recombinant Proteins		
6-Cyano-7-nitroquinoxaline-2,3-dione disodium salt hydrate (CNQX)	Sigma-Aldrich	Catalog # C239
D(-)-2-Amino-5-phosphonopentanoic acid (AP-5)	Sigma-Aldrich	Catalog # A8054
Picrotoxin (PTX)	Sigma-Aldrich	Catalog #P1675
BAPTA-AM	Abcam	Catalog # ab120503
Saclofen	Tocris	Catalog # 0246
U73122	Tocris	Catalog # 1268
CGP-55845 hydrochloride	Tocris	Catalog # 1248
Tetrodotoxin (TTX)	Enzo Life Sciences	Catalog # BML-NA120-0001
Transferrin	Calbiochem	Catalog # 616420
Cytosine Arabinoside (Ara-C)	Sigma	Catalog # C6645
B-27 supplement	GIBCO	Catalog # 17504-010
Experimental models: Cell lines		
Human embryonic kidney-293 (HEK293) cells	ATCC	Catalog # CRL-1573 RRID: CVCL_0045
Experimental Models: Organisms/Strains		
Sprague-Dawley rat pups (P2–P3)	Charles River	Strain code: 400
Heterozygous SNAP25Delta3 mice and WT littermates	Zurawski et al. Science Signaling 2019	N/A
Recombinant DNA		
Plasmid: pRSV-REV (lentiviral packaging)	Addgene	Catalog # 12253
Plasmid: pCMV-VSV-G (lentiviral packaging)	Addgene	Catalog # 8454
Plasmid: pMDLg/pRRE (lentiviral packaging)	Addgene	Catalog # 12251
Plasmid: pFUGW-ctGRK2	This paper	N/A
Plasmid: pFUGW-myr-ctGRK2	This paper	Addgene ID: 178734
Plasmid: Syt1-shRNA-mCherry	Gift from Sudhof lab	N/A
Plasmid: Syt1-WT	Gift from Sudhof lab	N/A
Plasmid: Syb2-GCaMP6s	This paper	N/A
Software and algorithms		
MiniAnalysis	Synaptosoft	http://www.synaptosoft.com/MiniAnalysis
Clampfit	Molecular Devices	http://www.moleculardevices.com
Axopatch	Molecular Devices	http://www.moleculardevices.com

REAGENT or RESOURCE	SOURCE	IDENTIFIER
Prism	GraphPad	http://www.graphpad.com
Mathlab	Mathworks	https://www.mathworks.com/products/matlab.html
Fiji	ImageJ processing package – open source	https://imagej.net/Fiji

Author Manuscript

Author Manuscript

Author Manuscript

Author Manuscript